# Calculation on viscous damping of deepwater catenary mooring line*

Qiao Dongsheng[1]，Ou Jinping[1,2]

1. School of Civil Engineering，Harbin Institute of Technology，Harbin China，150090

2. School of Civil and Hydraulic Engineering, Dalian University of Technology，

Dalian China，116024

## Abstract

Abstract: Viscous damping due to drag on deepwater catenary mooring line is significantly affected by a floating platform. The absorption of energy by a mooring line from the floating platform as a result of its motion is applied to calculate the viscous damping of the mooring line. The calculation model is a wire line in deepwater from a report of the International Ship and Offshore Structures Congress (ISSC), Committee I2 at Trondheim, Norway in 1997. The mooring line and seabed interaction is based on the hypothesis of rigid seabed. The fluid drag force and inertia force on the mooring line are calculated according to the Morrison formula. Respectively under the hydrostatic condition and the velocity distribution condition, the mooring line non-liner dynamic analysis is executed in the time-domain based on the finite element method. Bi-harmonic floating platform oscillations which combine wave and drift induced excitation are specified, meanwhile they represent the wave drift motion, the wave frequency motion and the combination of them. The maximum tension in the mooring line and the viscous damping are obtained from the results. Through this study, predictions of the dynamic tension and the viscous damping induced by the mooring line on time-domain finite element methods are proved feasible.

**Keywords:** Deepwater catenary mooring system; viscous damping; absorbed energy; non-liner dynamic analysis

## Nomenclature

$M$ = structural mass

$M_a$ = added mass

$X$ = motion displacement

$t$ = time

$B$ = linear damping coefficient

$K(X)$ = mooring stiffness

$F$ = exciting force

$F_{Dt}$ = line tangential drag forces (per unit length)

$F_{Dt}$ = line tangential drag forces (per unit length)

$\rho_w$ = fluid density

$C_{Dt}$ = tangential drag coefficient

$D$ = wire diameter

$\Delta V_t$ = relative tangential velocity of the fluid

$F_{Dn}$ = line normal drag forces (per unit length)

$C_{Dn}$ = normal drag coefficient

$\Delta V_n$ = relative normal velocity of the fluid

$F_{It}$ = line tangential added mass forces (per unit length)

$C_{It}$ = tangential added mass coefficient

$a$ = line acceleration

$F_{In}$ = line normal added mass forces (per unit length)

$C_{In}$ = normal added mass coefficient

$E$ = dissipated energy

$\tau$ = one surge oscillation of period

$T$ = line upper end tension

$q$ = line upper end displacement

$X_0$ = amplitude of sinusoidal motion

## 1 Introduction

Since there is a need for energy sources, the deeper waters are more and more attended by people. The floating offshore platform are usually in position by multipoint mooring system which combined by multi-mooring lines. Mooring lines are typically a combination of wire and chain. Now, some polyester lines are also used in the taut-wire mooring system. The traditional catenary mooring system is usually designed to resist the horizontal forces of platform caused by the environmental loads. Meanwhile, the mooring lines are also suffering the environmental loads.

Damping is one of the most important factor in predicting the motion of a moored offshore platform. The main source of damping are current viscous flow effects, wind, wave drift and mooring line damping. The mooring line damping results from the line hydrodynamic drag with

*National 863 Plan Projects(2006AA09A103；2006AA09A104)

Author. Tel.: 15998484374. Email: qds903@163.com

possible vortex-induced vibration, line internal forces and the line friction on the seabed.

It is usually considered that the dominating line damping component is the line hydrodynamic drag. Previously reported work has shown that the mooring line damping should be calculated carefully and some work has down. Bauduin and Naciri [1] used MATLAB establish a quasi-static method to calculate the mooring line damping caused by floating platform low-frequency motion. Webster [2] used a time domain finite element approach to perform a parametric study of the mooring line damping induced by both horizontal and vertical top end motions. The parameters used in this analysis stem from a dimensional analysis. Brown and Mavrakos [3] presented a comparative study on mooring line dynamics and damping based on both time domain and frequency domain methods. Hwang [4] presented a time domain finite element model of the coupled dynamics of a floater and its mooring lines. The purpose of the model is to perform numerical decay tests from which mooring line damping coefficients may be derived. Kitney and Brown [5] presented two different scale experiments to validate the results of other scholar.

The International Ship and Offshore Structures Congress (ISSC), Committee I2 initiated a comparative study during the period 1994-1997 to perfect the dynamic analysis of moorings, and to assess the level of uncertainty in predicting the dynamic tension and mooring induced damping required for global analysis. In this paper, the calculation model is System II of the comparative study.

Yu Long and Tan Jiahua [6] presented a time-dominate dynamic finite element method to analysis the two-components mooring line. Also, the mooring line non-liner dynamic analysis in this paper is executed in the similar method.

This paper focus on the numerical simulation of the mooring line damping used a time-dominate dynamic finite element method. Respectively under the hydrostatic condition and the velocity distribution condition, bi-harmonic floating platform oscillations which combine wave and drift induced excitation are specified, meanwhile they represent the wave drift motion, the wave frequency motion and the combination of them. Then the maximum tension in the mooring line and the viscous damping are obtained from the results. Through this study, predictions of the dynamic tension and the viscous damping induced by the mooring line on time-domain finite element methods are proved feasible.

## 2 Calculation principle

Considering a mooring line, the surge or sway motion equation is governed by the following equation:

$$(M + M_a)\frac{d^2X}{dt^2} + B\frac{dX}{dt} + K(X)X = F \quad (1)$$

The definition of drag and added mass coefficients required careful consideration to ensure consistency between results. The definitions of mooring line tangential and normal drag forces (per unit length) used in the study are:

$$F_{Dt} = \frac{1}{2}\rho_w C_{Dt}\pi D\Delta V_t \left|\Delta V_t\right| \quad (2)$$

and

$$F_{Dn} = \frac{1}{2}\rho_w C_{Dn} D\Delta V_n \left|\Delta V_n \bullet \Delta V_n\right|^{1/2} \quad (3)$$

respectively. Line tangential and normal added mass forces (per unit length) are defined as:

$$F_{It} = \frac{1}{4}\rho_w \pi D^2 (C_{It} - 1)a \quad (4)$$

and

$$F_{In} = \frac{1}{4}\rho_w \pi D^2 (C_{In} - 1)a \quad (5)$$

The dissipated energy $E$ during one surge oscillation of period $\tau$ is given by:

$$E = \int_0^\tau T\frac{dq}{dt}dt \quad (6)$$

It if often convenient to express this damping in terms of an equivalent linear damping coefficient, $B$ . Then, the instantaneous value of $T$ can be approximated given by:

$$T = B\frac{dq}{dt} \quad (7)$$

If the motion is sinusoidal with an amplitude, $X_0$ , and a period, $\tau$ , the approximate absorbed energy $E$ is given by:

$$E = \int_0^\tau T\frac{dq}{dt}dt = B\int_0^\tau \left[\frac{dq}{dt}\right]^2 dt = \frac{2\pi^2 X_0^2 B}{\tau} \quad (8)$$

Consequently, provided the energy dissipated by the mooring line during one surge oscillation can be computed, the linear damping coefficient is obtained by:

$$B = \frac{E\tau}{2\pi^2 X_0^2} \quad (9)$$

The dissipated energy $E$ can be obtained by integrating the work done by the upper tension during one surge oscillation. This requires the use of a finite element dynamics program.

## 3 Calculation model and parameters

Analysis of a single line only was considered. No calculations were performed for wire/chain mixes. These are commonly used in the field but restricting calculations to single lines of wire or chain allows better interpretation and more general applicability of the results.

For each calculation set a base case was defined representing typical conditions. Variations about the base case were then considered.

### 3.1. calculation model

| Item | System 2 |
|---|---|
| Line type | Wire |
| Line diameter | 130 (mm)[c] |
| Total line length (unstretched) | 4000 (m) |
| Line weight (in air) | 800.5 (N/m)[c] |
| Line weight (in water) | 664.4 (N/m)[d] |
| Line axial stiffness EA | $1.30 \times 10^9$ (N)[c] |
| Line top tension at equilibrium position[a] | 1133.6 (kN) |
| Top end static horizontal offset - in positive x direction (see Fig. 1) | 50.0 (m) |
| Water depth | 500 (m) |
| Sea bed inclination | Horizontal |
| Sea bed friction coefficient | 0.0 |
| Current velocity | 0.0 (m/s) |

**Table 1:** Line physical properties and site conditions

The mooring physical properties and site conditions are defined in Table 1 with the line configuration depicted in Fig. 1. Water density of 1025 kg/m3 was used with the mooring line top end taken at the still water level as shown in Fig. 1. Contributions from the internal (structural) damping of the mooring line were ignored. Likewise, forces induced by in-plane and out-of-plane movement of the line on the seabed were not included.

Initial taut-catenary configuration was developed by using static steps [7] (Figure 2). The mooring lines were horizontally stretched out in their respective orientation by applying inline tension while keeping the fairlead fixed. Anchor end of the lines were then lowered to the seabed and horizontally positioned such that the desired pretension is achieved. Finally, the fairlead is released and verified that it is in static equilibrium at its mean position. Static and dynamic loads were then applied, as required by the analysis. This technique is more accurate because the stress and stiffness associated with the mean curvature of mooring lines are automatically included in the model.

Where time-domain-based calculations were performed these were run over simulation times corresponding to the larger of the imposed wave or wave drift motion period specified in the following section. Transients were eliminated by allowing a suitable start-up interval.

Dynamic model use beam element, the line tension induced by drag force is calculated by the whole tension minus the tension induced by the motion.

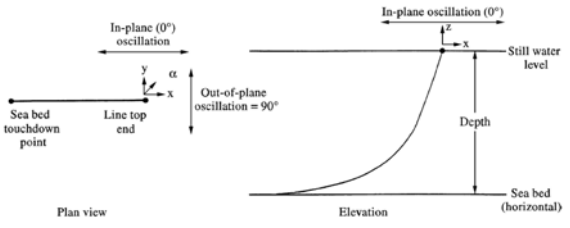


Fig. 1. Mooring line configuration (before static offset or loading applied).

**Figure 1:** Mooring line configuration (before static offset or loading applied).

### 3.2. calculation parameters

A base case set of loading conditions was defined and variations from the base case specified in Table 2.

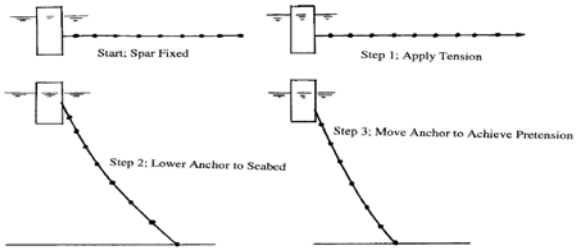


**Figure 2:** Static steps for initial catenary configuration.

| | | | |
|---|---|---|---|
| | | | |
| 1.1 | 30 | 330 | $q = 30\sin(\frac{2\pi}{330}t)$ |
| 1.2 | 50 | 330 | $q = 50\sin(\frac{2\pi}{330}t)$ |
| 1.3 | 5.4 | 10 | $q = 5.4\sin(\frac{2\pi}{10}t)$ |
| 1.4 | 9 | 10 | $q = 9\sin(\frac{2\pi}{10}t)$ |
| 1.5 | 30 | 200 | $q = 30\sin(\frac{2\pi}{200}t)$ |
| 1.6 | 5.4 | 5 | $q = 5.4\sin(\frac{2\pi}{5}t)$ |
| 1.7 | | | $q = 30\sin(\frac{2\pi}{330}t) + 5.4\sin(\frac{2\pi}{10}t)$ |
| 1.8 | | | $q = 30\sin(\frac{2\pi}{330}t) + 9\sin(\frac{2\pi}{10}t)$ |
| 2.1 | Current velocity 1.03m/s | | $q = 30\sin(\frac{2\pi}{330}t)$ |
| 2.2 | Current velocity 1.03m/s | | $q = 5.4\sin(\frac{2\pi}{10}t)$ |
| 2.3 | Current velocity 1.03m/s | | $q = 30\sin(\frac{2\pi}{330}t) + 5.4\sin(\frac{2\pi}{10}t)$ |

**Table 2:** Calculation parameters variation

# 4 Results

### 4.1. Maximum tension

Fig. 3 shows total (catenary plus dynamic) maximum tension over an oscillation cycle for systems 2. The term catenary tension refers to the fairlead static tension calculated from the classic catenary equations, associated

with the maximum fairlead translation for each test. Consequently no fluid dynamic loading effects are allowed for and the fairlead translation will include contributions from the static horizontal offset, together with the amplitude of motion associated with the imposed drift (d), the wave (w) or the combined wave/drift (w/d) motion. Line tensions from catenary theory are also given in the figures. Table 3 also provides mean and standard deviation values from time and frequency-domain calculations together with the catenary tension as defined above.

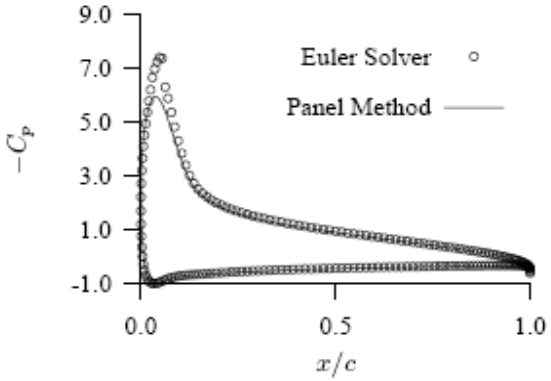


**Figure 3:** High-loaded NACA 0015 cascade of blades with $S/C$ = 1.5 at $\beta_m$ = 10.5º and $Ma_m$ = 0.32. Surface pressure distribution.

| | | | |
|---|---|---|---|
| 1.1 | 30 | 330 | $q = 30\sin(\frac{2\pi}{330}t)$ |
| 1.2 | 50 | 330 | $q = 50\sin(\frac{2\pi}{330}t)$ |
| 1.3 | 5.4 | 10 | $q = 5.4\sin(\frac{2\pi}{10}t)$ |
| 1.4 | 9 | 10 | $q = 9\sin(\frac{2\pi}{10}t)$ |
| 1.5 | 30 | 200 | $q = 30\sin(\frac{2\pi}{200}t)$ |
| 1.6 | 5.4 | 5 | $q = 5.4\sin(\frac{2\pi}{5}t)$ |
| 1.7 | | | $q = 30\sin(\frac{2\pi}{330}t) + 5.4\sin(\frac{2\pi}{10}t)$ |
| 1.8 | | | $q = 30\sin(\frac{2\pi}{330}t) + 9\sin(\frac{2\pi}{10}t)$ |
| 2.1 | Current velocity 1.03m/s | | $q = 30\sin(\frac{2\pi}{330}t)$ |
| 2.2 | Current velocity 1.03m/s | | $q = 5.4\sin(\frac{2\pi}{10}t)$ |
| 2.3 | Current velocity 1.03m/s | | $q = 30\sin(\frac{2\pi}{330}t) + 5.4\sin(\frac{2\pi}{10}t)$ |

**Table 3:** Maximum tension and mooring-induced damping

#### 4.2. Mooring-induced damping

Fig. 4 give calculated line damping values over an oscillation cycle of period q. Statistical results calculated from the set of contributor data are presented as for the tension amplitude values discussed above.

There is up to 60% variation about the mean for the time-domain linearized damping results as damping calculations depend on the line tension variation throughout the complete oscillation cycle. Results for the deep water wire system show wider variation.

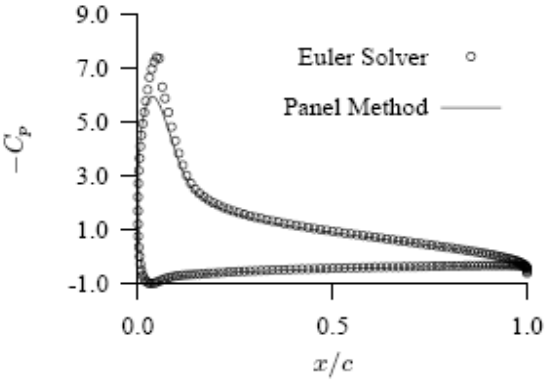


**Figure 4:** High-loaded NACA 0015 cascade of blades with $S/C$ = 1.5 at $\beta_m$ = 10.5º and $Ma_m$ = 0.32. Surface pressure distribution.

#### 4.3. Influence of motion amplitude

Figs. 5 and 6 give calculated line damping values over an oscillation cycle of period q. Statistical results calculated from the set of contributor data are presented as for the tension amplitude values discussed above.

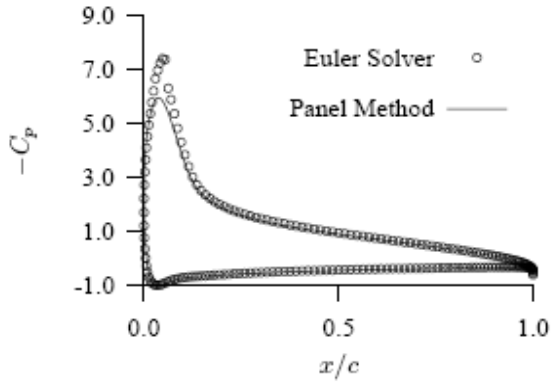


**Figure 5:** High-loaded NACA 0015 cascade of blades with $S/C$ = 1.5 at $\beta_m$ = 10.5º and $Ma_m$ = 0.32. Surface pressure distribution.

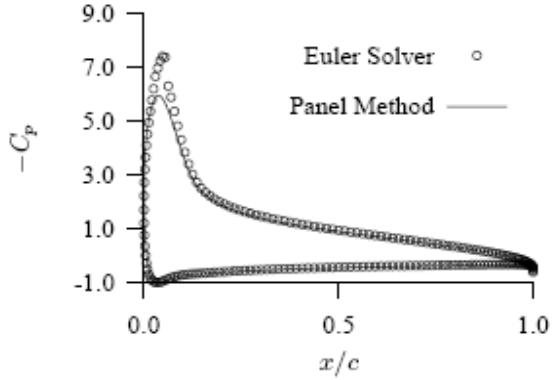


**Figure 6:** High-loaded NACA 0015 cascade of blades with $S/C$ = 1.5 at $\beta_m$ = 10.5º and $Ma_m$ = 0.32. Surface pressure distribution.

#### 4.4. Influence of motion period

Figs. 7 and 8 give calculated line damping values over an oscillation cycle of period q. Statistical results calculated from the set of contributor data are presented as for the tension amplitude values discussed above.

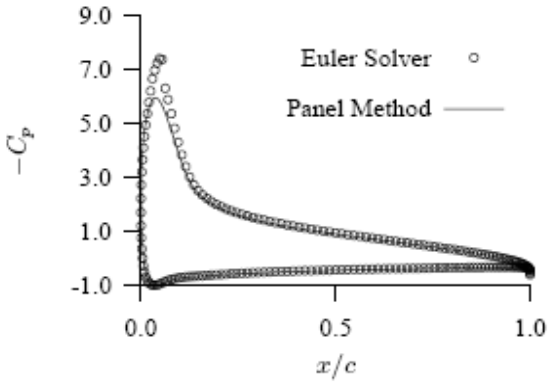


**Figure 7:** High-loaded NACA 0015 cascade of blades with $S/C$ = 1.5 at $\beta_m$ = 10.5º and $Ma_m$ = 0.32. Surface pressure distribution.

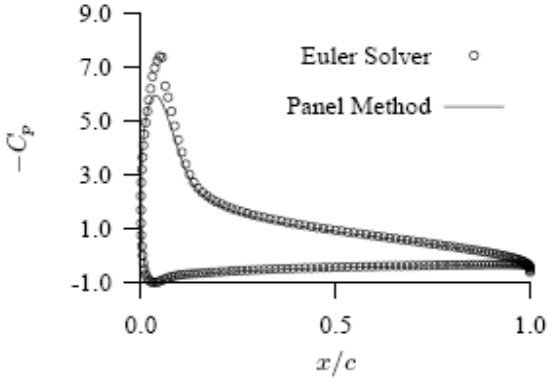


**Figure 8:** High-loaded NACA 0015 cascade of blades with $S/C$ = 1.5 at $\beta_m$ = 10.5º and $Ma_m$ = 0.32. Surface pressure distribution.

#### 4.5. Influence of current velocity

Figs. 9 and 10 give calculated line damping values over an oscillation cycle of period q. Statistical results calculated from the set of contributor data are presented as for the tension amplitude values discussed above.

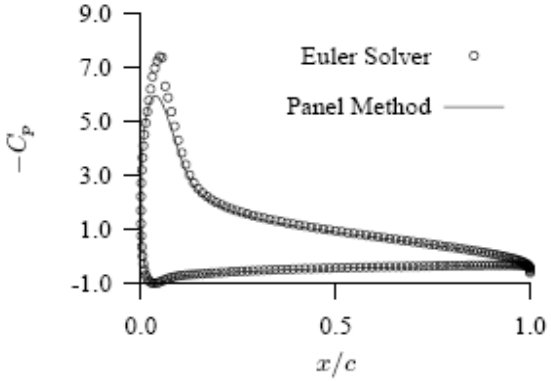


**Figure 9:** High-loaded NACA 0015 cascade of blades with $S/C$ = 1.5 at $\beta_m$ = 10.5º and $Ma_m$ = 0.32. Surface pressure distribution.

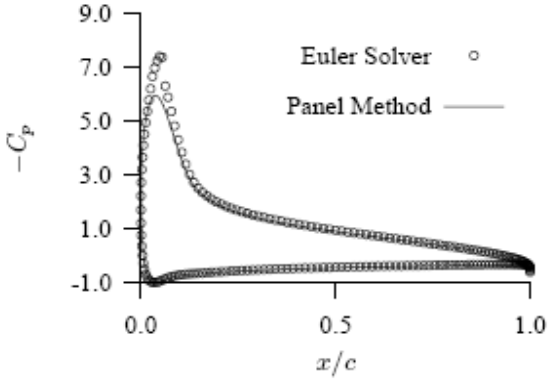


**Figure 10:** High-loaded NACA 0015 cascade of blades with $S/C$ = 1.5 at $\beta_m$ = 10.5º and $Ma_m$ = 0.32. Surface pressure distribution.

## 5 Conclusion


## Acknowledgements

Acknowledgements of people, grants, funds, etc should be placed in a separate section not numbered at the very end of the paper.


## References


[1] C. Bauduin and M. Naciri. A Contribution on Quasi-Static Mooring Line Damping. *Journal of Offshore Mechanics and Arctic Engineering*,122:125-133,2000

[2] W. C. Webster. Mooring-Induced Damping. *Ocean Engineering*, 22(6):571–591,1995

[3] D. T. Brown and S. Mavrakos. Comparative Study on Mooring Line Dynamic Loading. *Journal of Marine Structure*,12:131-151,1999

[4] Y. L. Hwang. Numerical Model Tests for Mooring Damping. *Proc. 17th OMAE Conference*,1998

[5] N. Kitney and D. T. Brown. Experimental Investigation of Mooring Line Loading Using Large and Small-Scale Models. *Journal of Offshore Mechanics and Arctic Engineering*,123:1-9,2001

[6] Yu Long and Tan Jiahua. Dynamics of two-components mooring line in deep water, *Journal of Jiangsu University of Science and Technology( Natural Science Edition)*,20(4):6-10,2006

[7] G. Chaudhury and Cheng-Yo Ho. Coupled Dynamic Analysis of Platforms, Risers, and Moorings, *OTC 12084 [C]*, 647-654, 2000